



# Imposing Constraints in a Full State Feedback System Using Multithreaded Controller

Marek Michalczuk , Member, IEEE, Bartłomiej Ufnalski , Senior Member, IEEE, and Lech Marian Grzesiak, Senior Member, IEEE

**Abstract**—The article proposes a ground-breaking solution to address the challenge of imposing constraints in a full state feedback (FSF) control system. Its simplicity is comparable to the introduction of saturation blocks in the cascaded control system. In the developed control system, a given state variable is stabilized at the threshold value using a separate FSF controller. The overall controller consists then of a set of controllers, the main one with an external reference signal and auxiliary controllers with the internal references set to the desired limits to be imposed on each of the physical states of the investigated plant, operating in parallel fashion (hence the proposed name—multithreaded). This means that in each time instance, the processor executes all FSF controllers. Additionally, if the auxiliary integral states are implemented, a back-calculation algorithm is employed to keep the auxiliary states at the desired level for the controllers that are idling at a given time instance. The median of the calculated control signals is put through to the plant as a control signal. Such an elegant and straightforward way of handling constraints in the state feedback system has never been reported before and is currently patent pending. The proposed method is validated for a servo drive using hardware-in-the-loop setup. All the obtained results confirm technical feasibility of the controller structure and its ability to keep all the state variables within the required intervals.

**Index Terms**—Constraints, electric drives, multithreaded state controller (MTSC), servo drives, state feedback controller.

## NOMENCLATURE

<b>A</b>	State matrix.
<b>B</b>	Input matrix.
<b>E</b>	Disturbance input matrix.
<b>x</b>	State vector.
$u_a$	Control signal proportional to armature voltage.
$\gamma$	Angular position of the rotor.

Manuscript received May 15, 2020; revised August 21, 2020 and November 2, 2020; accepted November 24, 2020. Date of publication December 21, 2020; date of current version August 25, 2021. This work was supported by the ENERGYTECH-1 project granted by the Warsaw University of Technology under the program Excellence Initiative: Research University (ID-UB). (Corresponding author: Marek Michalczuk.)

The authors are with the Institute of Control and Industrial Electronics, Faculty of Electrical Engineering, Warsaw University of Technology, 00-662 Warsaw, Poland (e-mail: marek.michalczuk@ee.pw.edu.pl; bartlomiej.ufnalski@ee.pw.edu.pl; lech.grzesiak@ee.pw.edu.pl).

Color versions of one or more figures in this article are available at <https://doi.org/10.1109/TIE.2020.3044778>.

Digital Object Identifier 10.1109/TIE.2020.3044778

$\omega$	Rotational speed of the rotor.
$m_L$	Load torque.
$m_e$	Torque developed by the machine.
$R_a$	Armature resistance.
$L_a$	Armature inductance.
$J$	Drive system momentum of inertia.
$\Psi$	Permanent magnet flux linkage.
$c_t$	Friction coefficient.
$K_{cnv}$	Converter voltage gain.

## I. INTRODUCTION

THIS study presents a new control approach for systems with full state feedback (FSF). The proposed method is original in terms of state variables and control signal limitation. In most cases, the control system for an electric drive besides fine reference tracking and disturbance rejection performance is subjected to dealing with nonlinearities. The most common nonlinearity met in practice is related with an actuator or the plant to be controlled itself. As for converter drives, the limited range of converter output voltage results in the limited range of the control signal. Additionally, care must be taken to restrict the motor current within a value that is safe for the motor, the power electronic system, and the source of energy. Furthermore, in the case of position control, attention should be paid to speed limitation. A control structure that does not support imposing limits usually cannot be used in an effective way, regardless of its potentially outstanding performance within the limits, i.e., in the linear region of the controller. The following approaches to constraints in electric drive systems can be distinguished.

- 1) Deterioration of the drive performance so constraints are not reached or alternatively exceedance is so short that is accepted.
- 2) The control design includes constraints from the beginning.
- 3) The design of the control system is performed disregarding the constraints and the constraints are added to the control structure *a posteriori*.

The first approach has a low implementation value because to get the most out of a system, one needs to push against the boundaries. In closed-loop drives requiring a fast response, the absolute value of motor speed or current can be intentionally forced to the maximum value in order to achieve a short rise time.

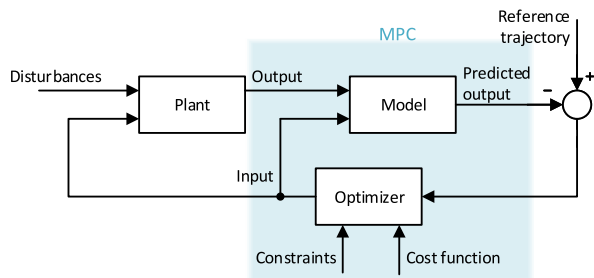


Fig. 1. Block diagram of MPC.

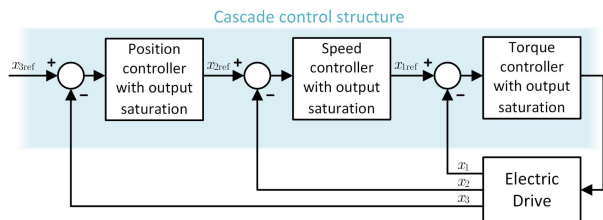


Fig. 2. Block diagram of cascade control.

In the second approach, the control design is performed directly by taking constraints into account. This approach includes model predictive control (MPC) [1]–[4]. The general concept of MPC is presented in Fig. 1. MPC has traditionally solved the optimization problem over a finite horizon using the receding horizon technique [5], [6]. MPC can take into account constraints of multiple input and multiple output plants. However, computation complexity of this method is high [7]–[9]. The optimization problem has to be solved in real time, which can pose implementation challenges, especially for applications with small time constants [10], [11].

The main advantage of the third approach, comparing to MPC, is smaller computation effort. The control design begins with the synthesis of a linear controller [12], [13]. Afterward, the effect of a constraint is taken on board and typically verified by simulation analysis. Among linear control systems for drives, two main types can be distinguished. The first type is a cascade control structure nesting several control loops. The general control scheme for an electric drive is shown in Fig. 2. Because a setpoint for each state variable is available in a cascade control structure ( $x_{1ref}$ ,  $x_{2ref}$ ,  $x_{3ref}$  in Fig. 2), a *posteriori* implementation of their restriction is very straightforward. It is done simply by limiting output signal for subsequent controllers, and the anti-windup mechanism if relevant, which is equivalent to limiting the reference signals for the controlled state variables. However, cascade control also has its drawbacks. Each additional inner-loop controller, other than the proportional one, increases the degree of the polynomial to be analyzed during the design of the consecutive outer-loop controllers, and that is also why many analytical design procedures circumvent this by simplifying the dynamics of the inner closed-loop subsystems. To make the cascade control effective, an inner control loop must react several times faster than the primary process reacts to the outer controller. This gives the inner controller enough time to compensate for inner-loop disturbances before they significantly

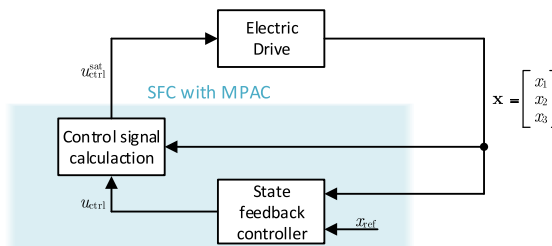


Fig. 3. Block diagram of MPACs.

affect the primary process [14]. Additionally, it is expected that the inner-loop disturbances are less harsh than the outer-loop disturbances. Otherwise, the outer controller will be constantly adjusting for disturbances to the inner loop and unable to apply consistent corrective efforts to the primary process [15].

Alternatively, another type of a linear control system, such as state feedback control (SFC), can be used. Theoretically, SFC gives full flexibility to design system closed-loop poles. Therefore, especially for systems with coupling between state variables, compared to the cascade control, SFC tends to give a better response in terms of both reference tracking and disturbance rejection. However, because there are no setpoint signals for internal states, the implementation of constraints is more complex than in the cascade structure. The proposal of constrained state feedback speed control for an electric drive, namely model predictive approach to constraint (MPAC), is presented in [16]. The ideal diagram of this concept is shown in Fig. 3. MPAC is a two-step design process. In the first step, a linear controller ignoring limitations is designed. Next, based on a discrete-time model of the drive system, constraints are added to the control system. A similar idea for an electric drive operated in a field-weakening region is presented in [17].

This article proposes a new approach to constrained state feedback control that does not require real-time computation of a system model to introduce constraints. The developed method gives the possibility to easily modify saturation thresholds, just like for cascade control, and ensure good control properties that are characteristic for SFC. Because our method uses several blocks operating in different threads, the name multithreaded state controller (MTSC) is proposed. For full clarity, it should be added that the method name has nothing to do with how the algorithm is performed by a CPU, i.e., it can be implemented as a single-threaded process, which is the case in our experimental verification.

This study demonstrates MTSC for a permanent magnet (PM) dc machine. The bulk of ac machine control systems is conceptually based on dc machine control [18], [19]. Thus, MTSC can also be adapted to drive systems with other types of electric machines. This article is organized as follows. Section II outlines the drive system with a dc motor and its mathematical description. The novel controller structure is described in Section III. Numerical studies in the continuous time domain are presented in Section IV. Section V examines digital implementation and verification of MTSC in an Hardware-in-the-loop (HIL) experiment. Section VI describes hardware-in-the-loop experiment. Finally, Section VII concludes this article.

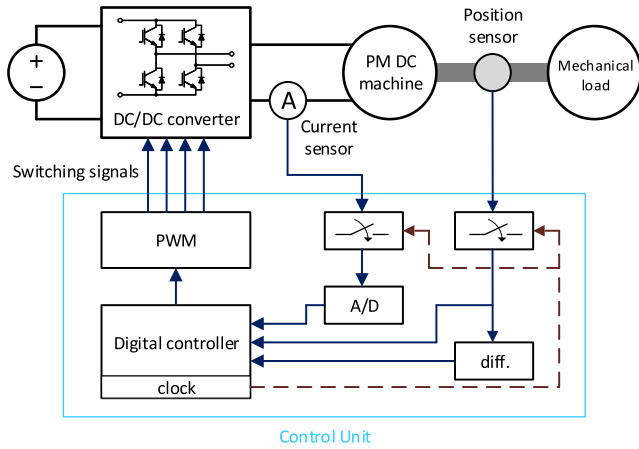


Fig. 4. Block diagram of the drive system.

 TABLE I  
DRIVE SYSTEM PARAMETERS

Parameter	Value	Parameter	Value
Nominal Power	370 W	Total inertia	5.7 kg cm <sup>2</sup>
Nominal motor speed	314 $\frac{\text{rad}}{\text{s}}$	Voltage constant	0.536 $\frac{\text{V}}{\text{rad}}$
Nominal load torque	1.08 N m	Maximum current	7.5 A
Input DC voltage	185 V	Maximum speed	314 $\frac{\text{rad}}{\text{s}}$
Nominal current	2.5 A	Switching frequency	20 kHz
Armature resistance	4.6 $\Omega$	Encoder resolutions	4096 ppr
Armature inductance	25 mH	Sample time	50 $\mu\text{s}$

## II. DRIVE SYSTEM

A schematic diagram of the drive system with a dc motor is shown in Fig. 4. The parameters of the system are listed in Table I. Motor parameters correspond to Lenze motor type of 13.120.65. The transform-based approach is used to design the controller. It is designed in the continuous time domain, using methods from continuous systems modeling and analysis. To implement this in a digital control system, a discretization method is used to get a discrete equivalent of the controller. The drive system, including the dc machine with the converter in the state space, is described by the following equation:

$$\frac{d}{dt}\mathbf{x} = \mathbf{A}_m\mathbf{x} + \mathbf{B}_m u + \mathbf{E}_m d \quad (1)$$

where

$$\mathbf{A}_m = \begin{bmatrix} -\frac{R_a}{L_a} & -\frac{\Psi}{L_a} & 0 \\ \frac{\Psi}{J} & -\frac{c_t}{J} & 0 \\ 0 & 1 & 0 \end{bmatrix}, \mathbf{B}_m = \begin{bmatrix} \frac{K_{\text{conv}}}{L_a} \\ 0 \\ 0 \end{bmatrix}, \mathbf{E}_m = \begin{bmatrix} 0 \\ \frac{1}{J} \\ 0 \end{bmatrix},$$

$$\mathbf{x} = \begin{bmatrix} i_a \\ \omega \\ \gamma \end{bmatrix}, u = u_a, \text{ and } d = m_{\text{load}}.$$

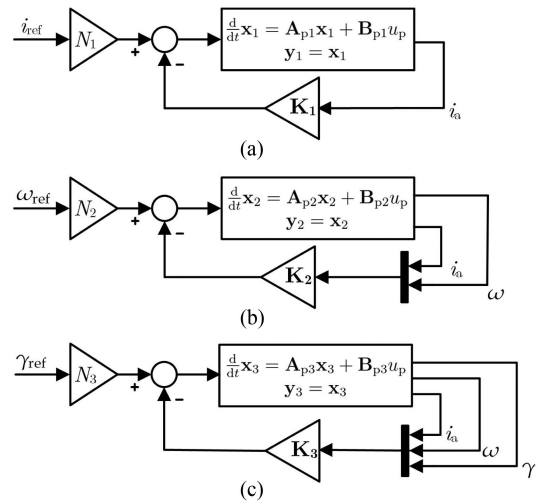


Fig. 5. Block diagram of linear state feedback controller. (a) Current controller. (b) Speed controller. (c) Position controller.

This article aims to validate a position controller with constraints on rotational speed, armature current, and control signal. The proposed method requires the design of three types of the state feedback controller with the possibility to stabilize each of the three state variables.

The plant to be controlled should be described in such a way that it is possible to control any state variable. To achieve this, variable  $i_a$  must be decoupled from  $\omega$ . Otherwise, armature current  $i_a$  could not be stabilized. The decoupling can be done by introducing new control variables as follows:

$$u_d = \Psi\omega \quad (2)$$

$$u_s = u_a - u_d. \quad (3)$$

After combining (2) and (3) with (1), the plant can be alternatively described as follows:

$$\frac{d}{dt}\mathbf{x} = \mathbf{A}_p\mathbf{x} + \mathbf{B}_p u_p + \mathbf{E}_p d \quad (4)$$

where

$$\mathbf{A}_p = \begin{bmatrix} -\frac{R_a}{L_a} & 0 & 0 \\ \frac{\Psi}{J} & -\frac{c_t}{J} & 0 \\ 0 & 1 & 0 \end{bmatrix}, \mathbf{B}_p = \mathbf{B}_m, \mathbf{E}_p = \mathbf{E}_m, \text{ and } u_p = u_s.$$

## III. CONTROL STRUCTURE

### A. Concept of Multithreading

For the object described by (4), it is possible to design SFCs for each state variable. The structures of controllers are presented in Fig. 5. The selection of  $\mathbf{K}_1$ ,  $\mathbf{K}_2$ ,  $\mathbf{K}_3$  and  $N_1$ ,  $N_2$ ,  $N_3$  can be done using well-established methods for linear systems, such as pole placement or linear-quadratic regulator (LQR). In practice, with the help of engineering tools, such as MATLAB, one gets the feedback gain directly by calling one function. The size of  $\mathbf{K}$  matrix for each controller depends on the number of state

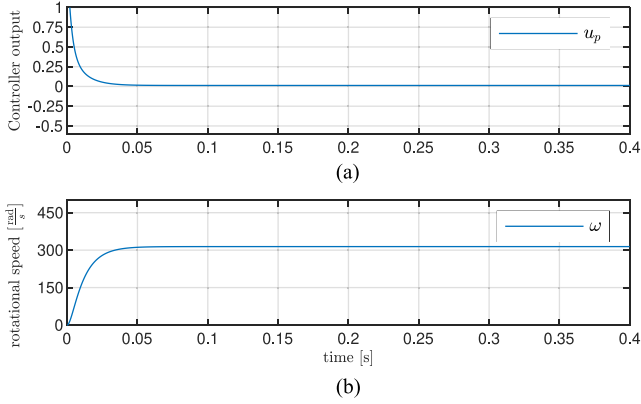


Fig. 6. Step response of linear speed controller [see Fig. 5(b)]. (a) controller output signal. (b) rotational speed.

variables. For design purposes of the position control, the plant is described by

$$\frac{d}{dt} \mathbf{x}_3 = \mathbf{A}_3 \mathbf{x}_3 + \mathbf{B}_3 u_p \quad (5)$$

where

$$\mathbf{A}_3 = \begin{bmatrix} -\frac{R_a}{L_a} & 0 & 0 \\ \frac{\Psi}{J} & -\frac{c_t}{J} & 0 \\ 0 & 1 & 0 \end{bmatrix}, \mathbf{B}_3 = \begin{bmatrix} \frac{K_{env}}{L_a} \\ 0 \\ 0 \end{bmatrix}, \text{ and } \mathbf{x}_3 = \begin{bmatrix} i_a \\ \omega \\ \gamma \end{bmatrix}.$$

For speed control, the plant is defined as follows:

$$\frac{d}{dt} \mathbf{x}_2 = \mathbf{A}_2 \mathbf{x}_2 + \mathbf{B}_2 u_p \quad (6)$$

where

$$\mathbf{A}_2 = \begin{bmatrix} -\frac{R_a}{L_a} & 0 \\ \frac{\Psi}{J} & -\frac{c_t}{J} \end{bmatrix}, \mathbf{B}_2 = \begin{bmatrix} \frac{K_{env}}{L_a} \\ 0 \end{bmatrix}, \text{ and } \mathbf{x}_2 = \begin{bmatrix} i_a \\ \omega \end{bmatrix}.$$

Similarly, for the current control task, the plant is represented as

$$\frac{d}{dt} \mathbf{x}_1 = \mathbf{A}_1 \mathbf{x}_1 + \mathbf{B}_1 u_p \quad (7)$$

where  $\mathbf{A}_1 = -\frac{R_a}{L_a}$ ,  $\mathbf{B}_1 = \frac{K_{env}}{L_a}$ , and  $\mathbf{x}_1 = i_a$ .

The idea of multithread control is based on the parallel determination of the control signal by each type of the controller. At any time, the selected control signal from parallel threads is given to the plant. The ideas of signal selection are shown in Figs. 6–8, on the example of speed limitation in position control. Therefore, for such a simplified case, let us consider two types of controllers: a position controller that accomplishes the main purpose of servo drive control and a speed controller with a set value equal to the upper threshold of rotational speed. The step responses of linear control systems are shown in Figs. 6 and 7. In this simplified two thread example, in each sample time, there is a need to select the control signal between the position controller and the speed controller. The choice of control signal is based on the following assumption: The speed response for the position control will not exceed the speed controller response if the control signal is not greater than the control signal determined

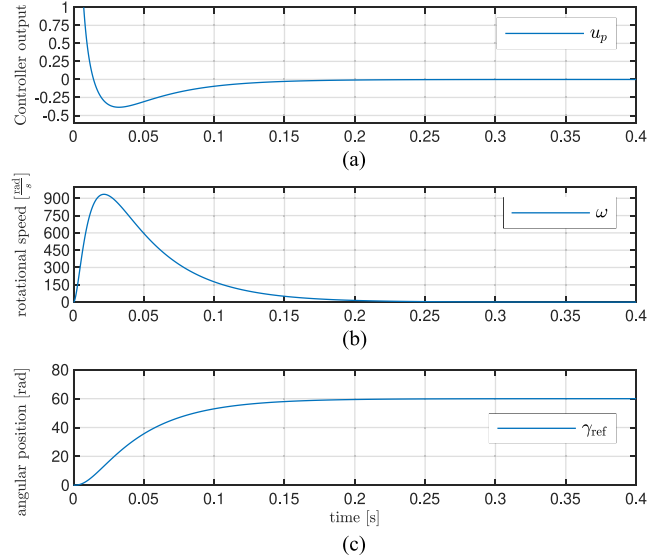


Fig. 7. Step response of linear position controller [see Fig. 5(c)]. (a) controller output signal. (b) rotational speed. (c) angular position.

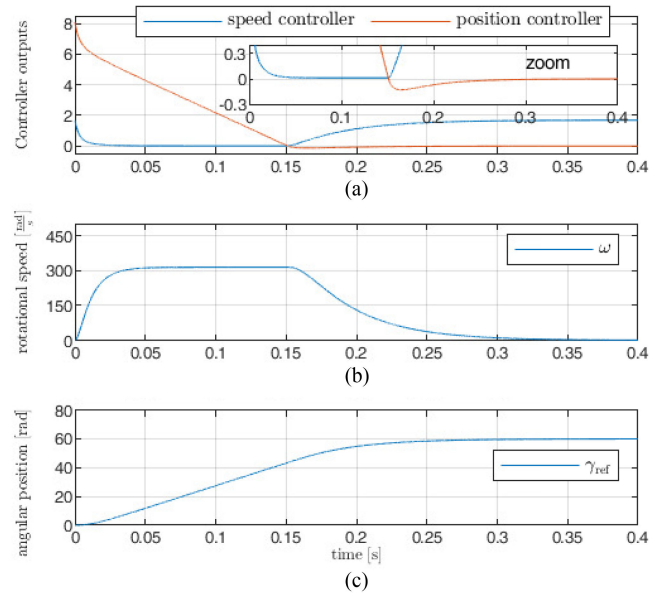


Fig. 8. Step response of position controller with speed saturation. (a) controllers output signals. (b) rotational speed. (c) angular position.

by the speed controller. As one can observe on the responses of linear systems, because the output signal from the position controller [see Fig. 7(a) in the initial phase has a higher value than the output signal from the speed controller [see Fig. 6(a)], the response of variable  $\omega$  in Fig. 7(b) is greater than the response shown in Fig. 6(b).

The operation of multithreaded control is illustrated in Fig. 8. In the initial phase, a signal from the speed controller is given to the plant. Thus, in the initial phase, the system response is analogous to response in Fig. 6. Around time 0.15s, the signal from the position controller drops below the signals from the speed controller and a signal from the position controller is passed to the plant. From that point on, the system goes to the

set position with the dynamics appropriate for position control, the same as in Fig. 7.

The same reasoning as presented for speed limitation can be applied to other state variables, and the presented two thread control can be extended for multithreaded control. Consequently, if for each internal variable two (upper and lower) thresholds are used, there are, beside the main position controller, two additional concurrently running controllers per each internal variable and the median of controller outputs should be provided as a control signal to the plant. More details on the multithreaded control structure are provided in Section III-C.

### B. Plant Augmentation

In accordance with the internal model principle, in order to compensate for constant disturbances, the controller structure should be augmented with integration of control error [20]–[23]. Accordingly, neglecting disturbances for controller design purposes, the plant is described as follows:

for the current controller

$$\frac{d}{dt} \begin{bmatrix} \mathbf{x}_1 \\ \rho_\omega \end{bmatrix} = \begin{bmatrix} \mathbf{A}_1 & 0 \\ 1 & 0 \end{bmatrix} \begin{bmatrix} \mathbf{x}_1 \\ \rho_\omega \end{bmatrix} + \begin{bmatrix} \mathbf{B}_1 \\ 0 \end{bmatrix} u_s \quad (8)$$

for the speed controller

$$\frac{d}{dt} \begin{bmatrix} \mathbf{x}_2 \\ \rho_\omega \end{bmatrix} = \begin{bmatrix} \mathbf{A}_2 & 0 \\ 0 & 1 \end{bmatrix} \begin{bmatrix} \mathbf{x}_2 \\ \rho_\omega \end{bmatrix} + \begin{bmatrix} \mathbf{B}_2 \\ 0 \end{bmatrix} u_s \quad (9)$$

for the position controller

$$\frac{d}{dt} \begin{bmatrix} \mathbf{x}_3 \\ \rho_\gamma \end{bmatrix} = \begin{bmatrix} \mathbf{A}_3 & 0 \\ 0 & 0 & 1 & 0 \end{bmatrix} \begin{bmatrix} \mathbf{x}_3 \\ \rho_\gamma \end{bmatrix} + \begin{bmatrix} \mathbf{B}_3 \\ 0 \end{bmatrix} u_s \quad (10)$$

### C. Multithreaded State Controller

As mentioned earlier, the idea of the operation of the MTSC is that as distinct from classic state feedback position control, there are additional concurrently running state feedback controllers of speed and current. The setpoints for additional controllers are the thresholds for a given state variable. The diagram of MTSC is shown in Fig. 9. The proposed control method uses five concurrently operated controllers with state feedback. These controllers are as follows.

- 1) Armature current controllers C1 and C2. The setpoints are maximum current  $i_{\max}$  for C1 and minimum current  $i_{\min}$  for C2 (the output signals are  $u_{i\max}$  and  $u_{i\min}$ , respectively),
- 2) Angular speed controllers C3 and C4. The setpoints are maximum speed  $\omega_{\max}$  for C3 and minimum speed  $\omega_{\min}$  for C4 (the output signals are  $u_{\omega\max}$  and  $u_{\omega\min}$ , respectively),
- 3) Angular position controller C5. The setpoint is the desired position  $\gamma_{\text{ref}}$  (the output signal is  $u_\gamma$ ).

The general schematic diagram of the controllers from C1 to C5 is shown in Fig. 10. Table II presents a description of signals corresponding to the controllers shown in Fig. 9. At the stage of selecting feedback gain matrix  $\mathbf{K}$  and feedforward gain

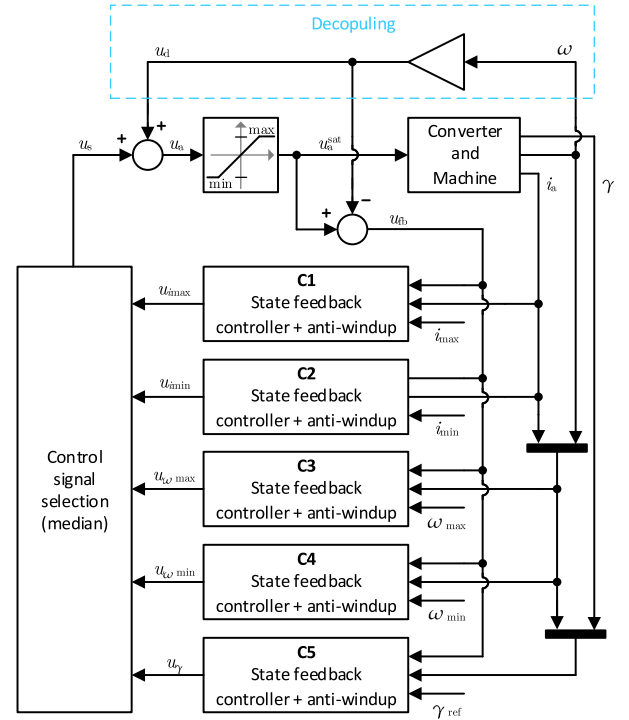


Fig. 9. Block diagram of MTSC for position control.

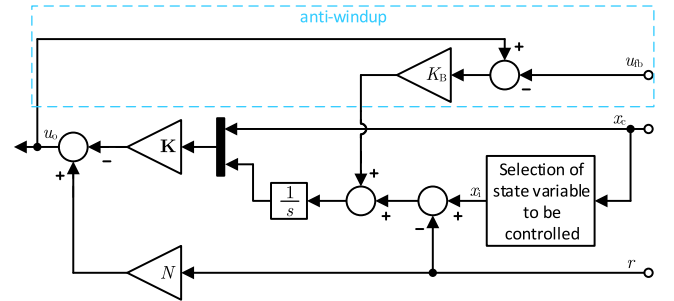
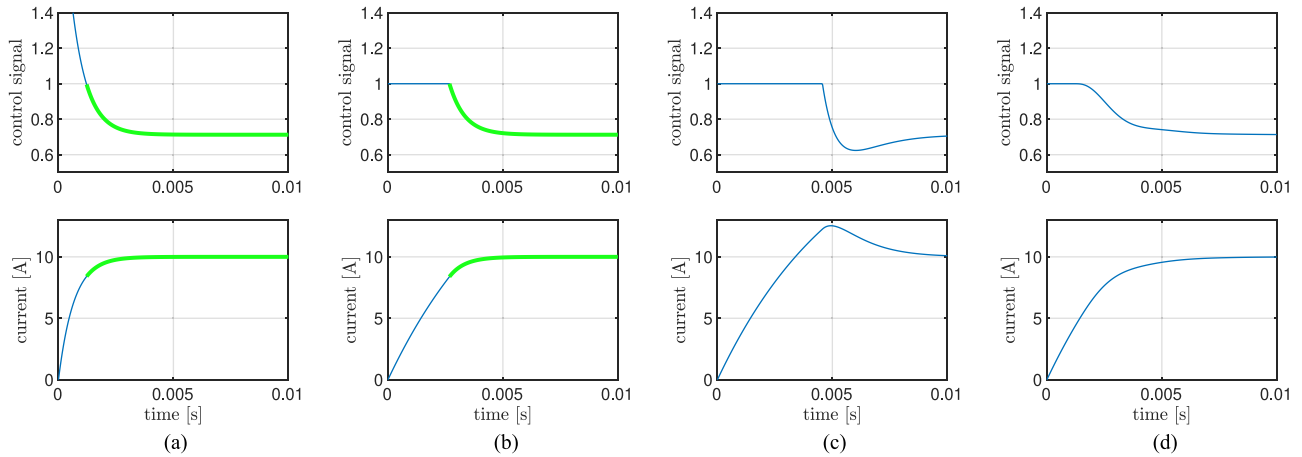


Fig. 10. Block diagram of a state feedback controller.

TABLE II  
SIGNAL DESCRIPTION FOR CONTROLLERS FROM C1 TO C5

Symbol in Fig.10	Controller C1	Controller C2	Controller C3	Controller C4	Controller C5
$u_o$	$u_{i\max}$	$u_{i\min}$	$u_{\omega\max}$	$u_{\omega\min}$	$u_\gamma$
$x_c$	$\begin{bmatrix} i_a \end{bmatrix}$	$\begin{bmatrix} i_a \end{bmatrix}$	$\begin{bmatrix} i_a \\ \omega \end{bmatrix}$	$\begin{bmatrix} i_a \\ \omega \end{bmatrix}$	$\begin{bmatrix} i_a \\ \omega \\ \gamma \end{bmatrix}$
$x_i$	$i_a$	$i_a$	$\omega$	$\omega$	$\gamma$
$r$	$i_{\max}$	$i_{\min}$	$\omega_{\max}$	$\omega_{\min}$	$\gamma_{\text{ref}}$
$\mathbf{K}$	$\mathbf{K}_i$	$\mathbf{K}_i$	$\mathbf{K}_\omega$	$\mathbf{K}_\omega$	$\mathbf{K}_\gamma$
$N$	$N_i$	$N_i$	$N_\omega$	$N_\omega$	$N_\gamma$
$K_B$	$K_{Bi}$	$K_{Bi}$	$K_{B\omega}$	$K_{B\omega}$	$K_{B\gamma}$





**Fig. 11.** Comparative analysis of anti-windup operation. (a) Theoretical response for a system without saturation. (b) Desired response for control signal saturation (green bold parts are identical). (c) Response for too low  $K_B$ . (d) Response for too high  $K_B$ .

$N$ , the linearity of the plant is assumed and the anti-windup mechanism is ignored.  $\mathbf{K}$  and  $N$  are chosen to obtain the desired response characteristic and an exemplary design procedure will be presented in Section IV. The selection of back-calculation anti-windup gain  $K_b$  will be justified in Section III-D.

The control signal  $u_s$  is one of the output signals from controllers C1 to C5, which is chosen in the control signal selection block (CSSB, see Fig. 9). The idea of a multithreaded controller comes down to the following rules.

- 1) First, while a drive system is operating without exceeding the thresholds for speed and current,  $u_\gamma$  is provided as control signal  $u_s$ .
- 2) Second, when the drive system tends to get out of the desired operating range, i.e., an internal state variable is going to reach the threshold value, then the CSSB is changing output signal  $u_s$  to a control signal from the controller that stabilizes the given state variable on the threshold value.

For a typical drive system, there is no reason to limit the range of the  $u_s$  signal. However, due to the limited output voltage of the dc-dc converter, there is a need to saturate the  $u_a$  signal, which is proportional to the voltage applied to the motor by the drive converter. Assuming that  $u_a^{\text{sat}}$  is the result of saturation of the  $u_s$  signal, the effective share of the control signal applied to the plant can be calculated as follows [see (3)]:

$$u_{\text{fb}} = u_a^{\text{sat}} - u_d. \quad (11)$$

The back-calculation algorithm is needed to keep auxiliary states within controllers that at a given time operate in the open-loop manner at the level ensuring the following behavior: the response characteristic of the drive system for the time of operation with a given controller, i.e., while the output of the given controller is provided as  $u_s$ , should not be affected by the operation time with other controllers or time of limiting the control signal, as illustrated by the example in Fig. 11. This example focuses on the issue of limiting the control signal and operation of a current controller that keeps  $i_a$  at 10A. System responses for four cases are presented in Fig. 11. In all cases,  $\mathbf{K}_i$  and  $N_i$  are the same. Fig. 11(a) shows the system response

when  $u_{i_{\text{max}}}$  is selected in CSSB and any saturation of the control signal is applied. Fig. 11(b) shows the desired response for operation with a control signal saturation. Until time equals 2.7ms, a saturated control signal is given to the plant. Next,  $u_{i_{\text{max}}}$  goes as a control signal and operation mode turns into current control. From that time on, the response is the same as in the case presented in Fig. 11(a), as marked with a bold green line.

Fig. 11(c) and (d) shows system responses possible in this structure but not desired. In these two cases, the system response in a current control mode is not consistent with the response in Fig. 11(a). The differences result from a wrong value of the controller's integrator state at a time when the system goes to the current control mode. Fig. 11(c) illustrates a case when the value of the integrator state was too high, which caused too late transition to the current control mode in relation to the desired response in Fig. 11(b). As a consequence, there is an overshoot. Fig. 11(d) shows the case when the value of the integrating state is too low. Thus, the response is insufficiently fast. The described problem can be addressed through a relevant change of the integrator state by the back-calculation mechanism in order to obtain the correct system response. Similar reasoning as presented here is applied to the speed and current limitation.

#### D. Back-Calculation

Looking at the operation of controllers from C1 to C5, two states for each controller can be distinguished. The first when the  $u_{\text{fb}}$  signal equals the output of a given controller and the anti-windup circuit (see Fig. 10) does not affect the operation of the controller. For a single-input plant, a schematic diagram describing the system for this state is shown in Fig. 12(a), where the feedback gain matrix  $\mathbf{K}$  is defined as

$$\mathbf{K} = \begin{bmatrix} \mathbf{K}_x & K_I \end{bmatrix}. \quad (12)$$

If part of the feedback is combined with the plant, the system can be presented as Fig. 12(b), where

$$u_c = u_{p1} + u_x \quad (13)$$

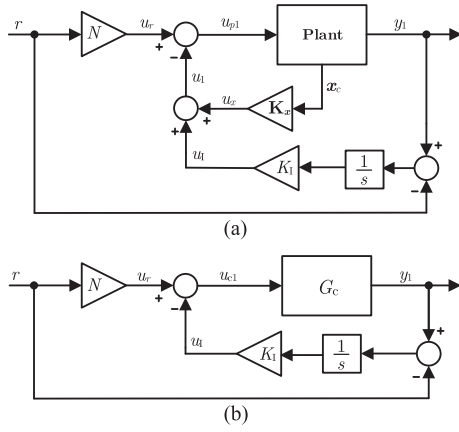


**Fig. 12.** Block diagram of the system with a state feedback controller in closed loop. (a) Block diagram of the system with a state feedback controller in closed loop. (b) Equivalent representation.

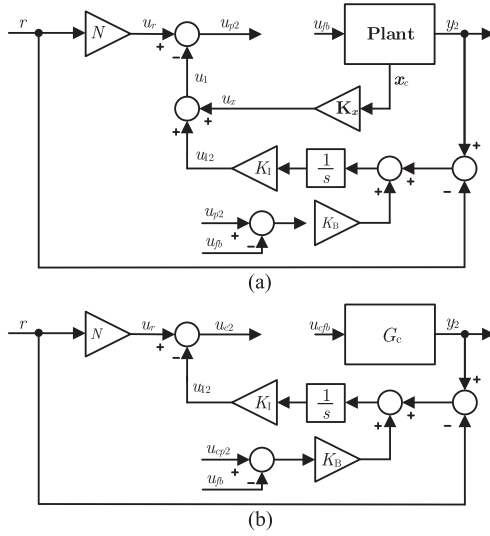


**Fig. 13.** Block diagram of the system with a state feedback controller in open loop. (a) Block diagram of the system with a state feedback controller in open loop. (b) Equivalent representation.

and

$$G_c(s) = \frac{u_{p1}(s)}{y_1(s)}. \quad (14)$$

Based on equations describing the system from Fig. 12

$$y_1 = G_c(Nr - u_1) \quad (15)$$

and

$$u_1 = K_I(y_1 - r) \frac{1}{s} \quad (16)$$

a transfer function  $G_I(s)$  can be determined

$$G_I(s) = \frac{u_1(s)}{y_1(s)} = -\frac{K_I - G_c K_I N}{G_c N s + G_c K_I}. \quad (17)$$

For the second state of controller C1 to C5, when the  $u_{fb}$  signal differs from the controller output signal, the block diagram is presented in Fig. 13(a). After similar combining of the part of the feedback, a scheme, as shown in Fig. 13(b), is obtained.

On the basis of Fig. 13, the  $u_{12}$  signal is described as follows:

$$u_{12} = K_I[(y_2 - r) + (u_{c2} - u_{fb})K_B] \frac{1}{s} \quad (18)$$

where

$$u_{c2} = Nr - u_{12}. \quad (19)$$

As outlined in the previous section, the aim of the anti-windup circuit is to keep the relation between  $u_{12}$  and  $y_2$  like between  $u_1$  and  $y_1$  in the case of the closed-loop mode (see Fig. 12). Thus, assuming the relationship

$$u_{12} = G_I y_2 \quad (20)$$

based on (18) and (19), one gets

$$K_B = \frac{(K_I(K_I r - u_{fb}s - G_c K_I u_{fb} + N r s))}{(K_I N (K_I r - u_{fb}s - G_c K_I u_{fb} + N r s))} = \frac{1}{N} \quad (21)$$

which means  $K_{Bi} = \frac{1}{N_i}$ ,  $K_{B\omega} = \frac{1}{N_\omega}$ , and  $K_{B\gamma} = \frac{1}{N_\gamma}$ . Such settings for the back-calculation gains provide the desired response of the system when a transition between two subcontrollers takes place.

#### IV. NUMERICAL STUDIES—CONTINUOUS SYSTEM ANALYSIS

The pole placement method is used to select  $K_i$ ,  $K_\omega$ , and  $K_\gamma$  feedback matrices. The object described by (4) and with parameters, as listed in Table I, has the following poles  $\lambda_p = [-184 \ -1.46 \ 0]$ . It was assumed that for a step change of the reference position, the response of the drive system should be aperiodic, and also the internal states should reach the threshold values in an aperiodic manner. For this reason, the poles of the closed loop are selected as real poles. The desired closed-loop poles depending on the type of controller are as follows.

- 1) For C1 and C2 controllers,  $\lambda_i = [-1.5 \cdot 10^3 \ -1.2 \cdot 10^3]$ .
- 2) For C3 and C4 controllers,  $\lambda_\omega = [-1.5 \cdot 10^3 \ -100 \ -80]$ .
- 3) For C5 controller,  $\lambda_\gamma = [-1.5 \cdot 10^3 \ -100 \ -50 \ -40]$ .

It is worth noting here that for a given state variable, the position of the associated pole does not depend on the type of controller. For each controller, the dominated pole related with the augmented state is set 25% lower than the slowest pole related with a machine state. Closed-loop poles are set based on the desired dynamic of the drive in a linear range. The selection of closed-loop poles is secondary here and has no impact on the idea of the proposed method. For example, in order to illustrate saturation of the control signal, the fastest pole is shifted to the left more than usual in drives.

The values of the feedforward gain  $N_i$ ,  $N_\omega$ , and  $N_\gamma$  are chosen in such a way to get a zero-pole cancellation for the dominant pole. Therefore

$$N_i = -\frac{K_i(2)}{\lambda_i(2)}, \quad N_\omega = -\frac{K_\omega(3)}{\lambda_\omega(3)}, \quad N_\gamma = -\frac{K_\gamma(4)}{\lambda_\gamma(4)}. \quad (22)$$

Fig. 14 presents the results of simulation tests, as well as the response of the drive system to step changes of reference angular position  $\gamma_{ref}$ . The results demonstrate full compliance with the expected behavior of the drive. The motor reaches the

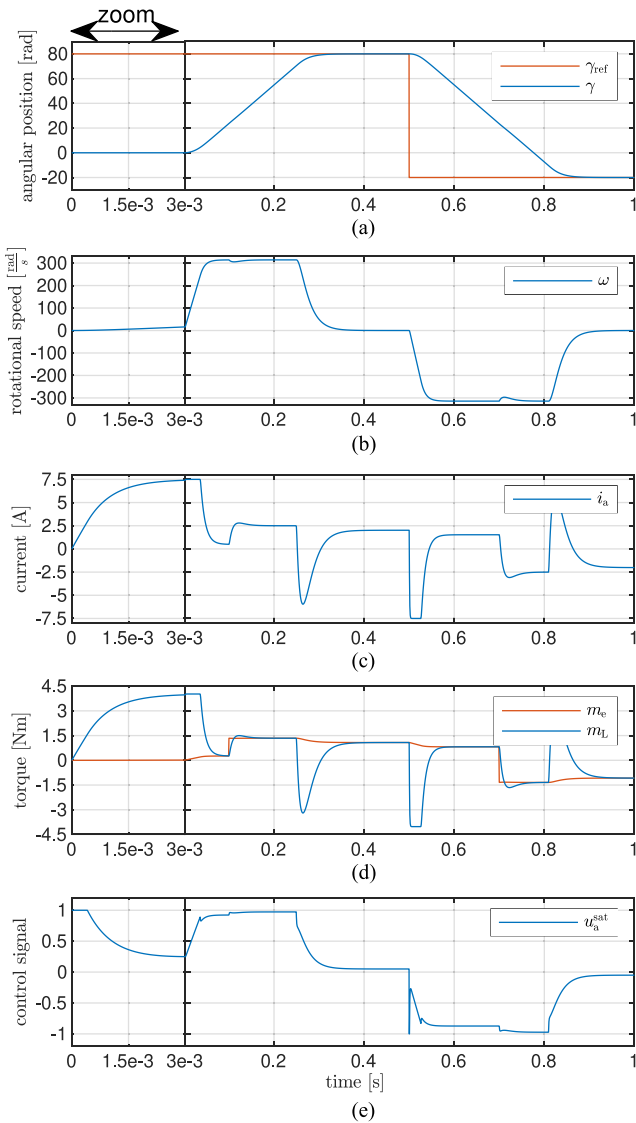


Fig. 14. Results of numerical study. (a) Reference and rotor position. (b) Rotational speed. (c) Armature current. (d) Load and motor torque. (e) Control signal.

setpoints with proper dynamics and correctly limits the speed and current in transient states. The obtained saturation levels of speed and current are equal to the predefined ones and each state variable reaches a threshold in an aperiodic manner. In order to clearly show the saturation of the control signal, the first 3ms is shown on a larger time scale. At time 0.1 and 0.7s, there are step changes of load torque. These tests demonstrate that the dynamics in terms of disturbance rejection is also very good.

The operation of the CSSB is presented in Fig. 15. The output signals for the cycle from Fig. 14 from all controllers from C1 to C5 are presented. The signal, which is a median, is marked with the bold line. The waveform obtained as a combination of all bold parts represents signal  $u_s$ .

## V. COMPARISON TO THE CLASSICAL METHOD

A comparison study has been performed in order to indicate differences between the classical method and the proposed

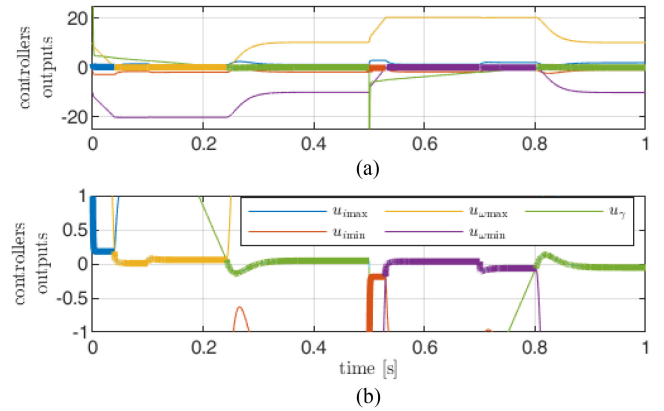


Fig. 15. (a) Illustration of CSSB operation. (b) Zoomed in.

MTSC. Fig. 16 presents comparative results of a servo drive system with classical cascade control structure [24], [25] and MTSC. The cascade control consists of proportional controller in the position control loop and proportional-integral controllers in speed and current control loops. Simulation results illustrate the response of servo drive for a step change in the commanded position (from 0 to 80rad). At time 0.1s, a step change of load torque is applied. Additionally, a step disturbance occurs in time 0.02s on the control signal. This type of disturbance is not typical for electric drives, but a response for that illustrates a good resemblance to how the control system deals with an inaccuracy of parameter identification.

In the first case presented in Fig. 16(a), the controllers are tuned in such a manner that the zero of PI controller compensates a dominant pole of the plant to be controlled and the dynamics of particular control loops are the same as dynamics of corresponding control threads in MTSC, namely the dominant pole of the compared closed-loop systems is in the same location in the  $s$ -plane. This approach allows to obtain the same character of the response for the classical system and the proposed MTSC, in terms of reference tracking, including reaching the threshold values of internal state variables [see Fig. 16(a) and (c)]. However, the classical cascade control system is much worse in terms of disturbance rejection.

For the following case presented in Fig. 16(b), the gains of controllers were increased to obtain the same time of disturbance rejection as in the system with MTSC in Fig. 16(c). Better dynamics of disturbance rejection comes at a cost of not so good response in terms of reaching the threshold values as well as high control cost expressed as high rms value of current.

The proposed MTSC method allows to effectively impose constraints and use the advantages of FSF, which enables to obtain high quality in terms of both reference tracking and disturbance rejection. Additionally, the MTSC enables independent shaping of the dynamics for the main thread FSF controller and for the FSF controllers with limits as the references. Note that this feature is not available in the cascade control system in which the dynamics of the inner-loop shapes the response collectively for saturated and nonsaturated reference value for the state variable controlled in the outer loop.



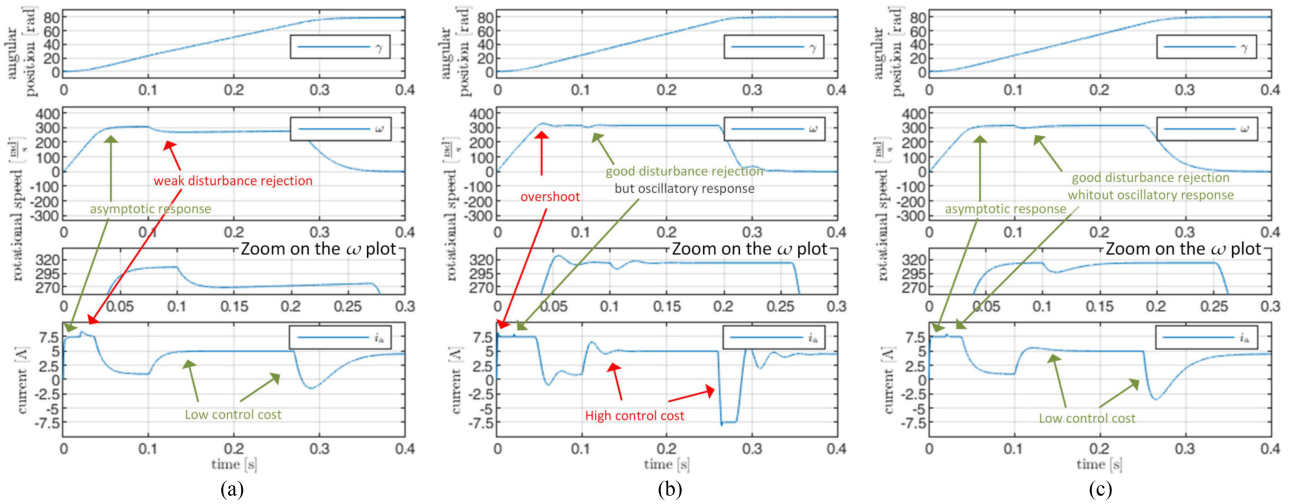


Fig. 16. Simulation results for the drive system with (a) cascade control structure—case 1, (b) cascade control structure—case 2, and (c) multithreaded control.

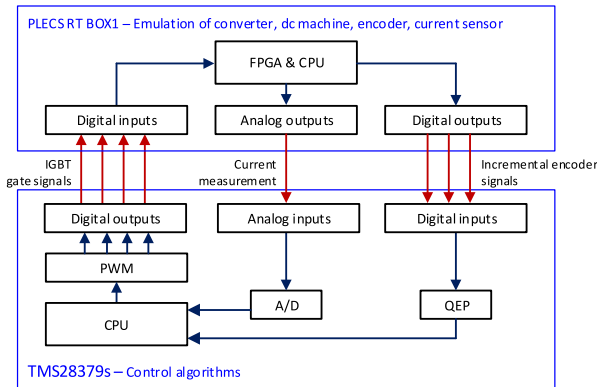


Fig. 17. Functional diagram of hardware-in-the-loop experiment.

### VI. HARDWARE-IN-THE-LOOP EXPERIMENT

The hardware-in-the-loop experiment is an acknowledged method to test a control system. In the experiment, the control algorithm runs in real time on an embedded controller potentially built into the final product. Because the controller responds not to a simulation signal, but to a real hardware signal, this type of verification provides very reliable results. The aim of the experiment presented here is to corroborate the possibility of practical implementation and investigate the potential effect of sampling on the plant. Plects RT BOX unit and digital signal processor (DSP) TMS320f28379s are used in the experiment. The functional diagram of hardware setup for the HIL experiment is shown in Fig. 17.

It should be noted that the implementation of the control algorithm on a physical controller is associated with some additional challenges. First, care is must be taken to consider a delay in the control loop. The loop delay of one sample period arises naturally from the nonzero processing time of physical DSP. The second complication concerns the quantization of measurement signals. This is particularly intense in the case of position measurement, because typically in electric drives,

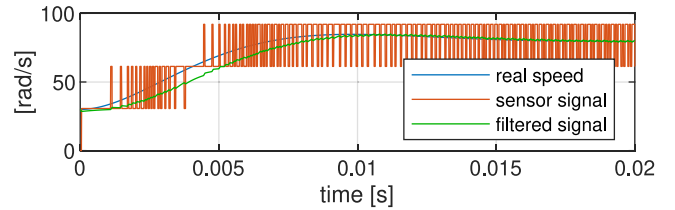


Fig. 18. Example plots of real signal, sensor signal, and filtered sensor signal for rotational speed.

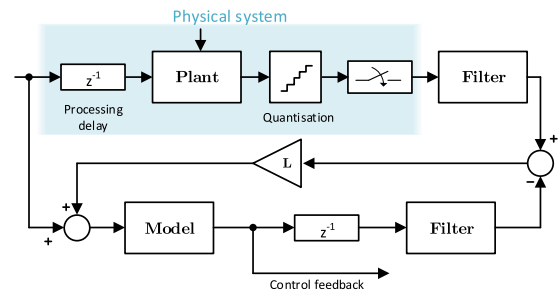


Fig. 19. Block diagram of state estimator.

the speed is determined by the difference quotient based on the position signal. The problem is presented in Fig. 18. In practice, the speed signal calculated as a difference quotient (red line in Fig. 18) has low resolution and it is insufficient to use this signal as feedback for a high-performance electric drive. Thus, obtaining the speed feedback based on a position encoder requires signal filtration. A typical low pass filter introduces some delay to the measurement signal (green line in Fig. 18). In this study, a low pass filter with cutoff frequency of 160Hz is used. As it is shown, feedback signals do not reflect  $\omega$  accurately at a given time. Because of this, a state observer is used in order to apply a control system with state feedback. The idea of the estimator based on the Luenberger observer is shown in Fig. 19. It may be mentioned that for the estimator,

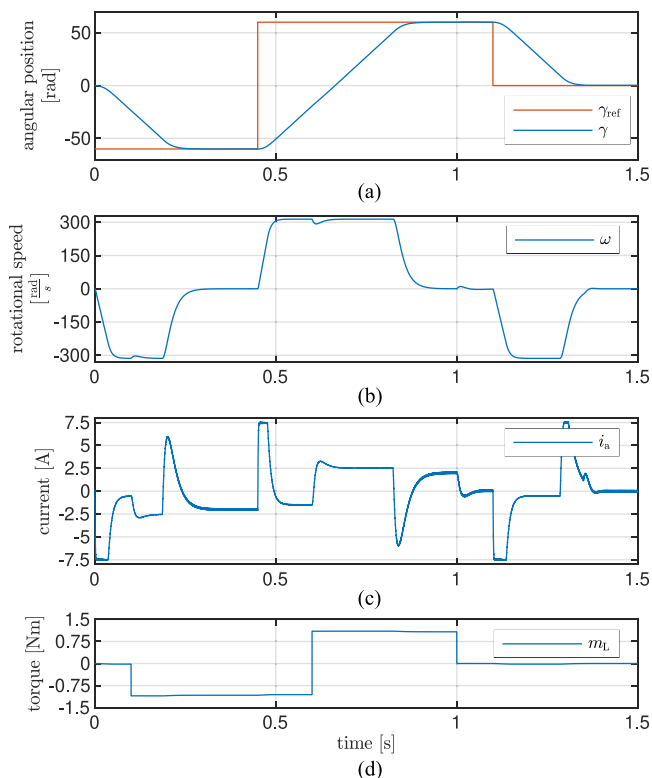


Fig. 20. Results of experiment study. (a) Reference and rotor position. (b) Rotational speed. (c) Armature current. (d) Load torque.

the presence of the delay is important, not its location before or after the plant model. Therefore, placing a delay on the model output instead of input is not an omission, but it is intentional to allow for compensation of the delay. This method of time delay compensation is known as Smith predictor [26]–[28].

The experiment results of MTSC operation for a servo drive with a PM dc machine are presented in Fig. 20. The commanded position and drive response are shown in Fig. 20(a). The absolute value of speed and current is effectively limited as assumed at  $314 \frac{\text{rad}}{\text{s}}$  and 7.5A, respectively, as shown in Fig. 20(b) and (c). In the test, the drive was subjected to a load torque, as presented in Fig. 20(d). The compensation of the load torque done by MTSC takes place as expected.

A good agreement between simulation results and experimental results for the physical controller has been obtained. Overall, these results indicate that MTSC can provide high-quality control, for which SFCs are known and at the same time provide an effective method to handle constraints.

## VII. CONCLUSION

An elegant and straightforward solution to the main challenge of the FSF controller was provided in this article. FSF was considered to be the gold standard of control systems from the theoretical point of view regarding unconstrained control. In FSF systems, the disturbance rejection versus reference tracking tradeoff was solved much more effectively in comparison to the cascade control systems. However, cascade control systems were at this point much more popular among practitioners that

by nature always deal with constrained control problems. From now on, it is equally easy to impose limits on state variables in FSF as in the cascaded control structure. This makes FSF a practical alternative and in fact superior to cascade control, because the main advantage of the cascade control, namely its ability to be easily modified into constrained control, has just been matched in FSF while keeping all other advantages. This gave us a very good candidate for the gold standard of control systems also from the practical point of view, i.e., regarding constrained control. The proposed MTSC was implemented on a DSP and successfully examined in an HIL experiment regarding a dc servo drive. The developed method can be applied in systems where state feedback controllers were commonly used whenever constrained control was required. It can also be used to replace controllers in applications currently dominated by cascade control structures in order to improve their performance.

## REFERENCES

- [1] S. Vazquez, J. Rodriguez, M. Rivera, L. G. Franquelo, and M. Norambuena, "Model predictive control for power converters and drives: Advances and trends," *IEEE Trans. Ind. Electron.*, vol. 64, no. 2, pp. 935–947, Feb. 2017.
- [2] C. Jia, X. Wang, Y. Liang, and K. Zhou, "Robust current controller for IPMSM drives based on explicit model predictive control with online disturbance observer," *IEEE Access*, vol. 7, pp. 45898–45910, 2019.
- [3] Z. Sun, Y. Zhang, S. Li, and X. Zhang, "A simplified composite current-constrained control for permanent magnet synchronous motor speed-regulation system with time-varying disturbances," *Trans. Inst. Meas. Control*, vol. 42, no. 3, pp. 374–385, 2020.
- [4] K. Lee, J. Lee, and Y. I. Lee, "Robust model predictive speed control of induction motors using a constrained disturbance observer," *Int. J. Control, Autom., Syst.*, vol. 18, no. 6, pp. 1539–1549, 2020.
- [5] F. Allgöwer and A. Zheng, *Nonlinear Model Predictive Control* (Progress in Systems and Control Theory), vol. 26. Basel, Switzerland: Birkhäuser Verlag, 2000.
- [6] R. Findeisen, and F. Allgöwer, "An introduction to nonlinear model predictive control," in *Proc. 21st Benelux Meeting Syst. Control*, 2002, vol. 11, pp. 119–141.
- [7] B. Stellato, T. Geyer, and P. J. Goulart, "High-speed finite control set model predictive control for power electronics," *IEEE Trans. Power Electron.*, vol. 32, no. 5, pp. 4007–4020, May 2017.
- [8] L. G. Bleris and M. V. Kothare, "Real-time implementation of model predictive control," in *Proc. Amer. Control Conf.*, 2005, vol. 6, pp. 4166–4171.
- [9] P. Karamanakos, E. Liegmann, T. Geyer, and R. Kennel, "Model predictive control of power electronic systems: Methods, results, and challenges," *IEEE Open J. Ind. Appl.*, vol. 1, pp. 95–114, Aug. 2020, doi: 10.1109/OJIA.2020.3020184.
- [10] V. Blasko, "Universal optimal model predictive control of multi-phase ac converters," in *Proc. IEEE 17th Workshop Control Model. Power Electron.*, Jun. 2016, pp. 1–7.
- [11] T. Geyer, *Model Predictive Control of High Power Converters and Industrial Drives*. New York, NY, USA: Wiley, 2016.
- [12] M. L. Corradini, A. Cristofaro, F. Giannoni, and G. Orlando, *Control Systems With Saturating Inputs: Analysis Tools and Advanced Design*, vol. 424. Berlin, Germany: Springer, 2012.
- [13] C. Brosilow and B. Joseph, *Techniques of Model-Based Control*. Englewood Cliffs, NJ, USA: Prentice-Hall, 2002.
- [14] R. Isermann, *Cascade Control Systems*. Berlin, Germany: Springer, 1991, pp. 49–55.
- [15] V. Vandoren, Fundamentals of cascade control, August 17, 2014, Accessed: Oct. 21, 2020. [Online]. Available: <https://www.controleng.com/articles/fundamentals-of-cascade-control>
- [16] T. Tarczewski and L. M. Grzesiak, "Constrained state feedback speed control of PMSM based on model predictive approach," *IEEE Trans. Ind. Electron.*, vol. 63, no. 6, pp. 3867–3875, Jun. 2016.
- [17] V. Šmídl, Š. Janouš, L. Adam, and Z. Peroutka, "Direct speed control of a PMSM drive using SDRE and convex constrained optimization," *IEEE Trans. Ind. Electron.*, vol. 65, no. 1, pp. 532–542, Jan. 2018.
- [18] N. P. Quang and J.-A. Ditttrich, *Vector Control of Three-Phase AC Machines*, 2nd ed. Berlin, Germany: Springer, 2015.

- [19] J. Pyrhonen, V. Hrabovcova, and R. S. Semken, *Electrical Machine Drives Control: An Introduction*. New York, NY, USA: Wiley, 2016.
- [20] M. A. M. Cheema, J. E. Fletcher, M. F. Rahman, and D. Xiao, "Optimal, combined speed, and direct thrust control of linear permanent magnet synchronous motors," *IEEE Trans. Energy Convers.*, vol. 31, no. 3, pp. 947–958, Sep. 2016.
- [21] L. Grzesiak and T. Tarczewski, "PMSM servo-drive control system with a state feedback and a load torque feedforward compensation," *Int. J. Comput. Math. Elect. Electron. Eng.*, vol. 32, no. 1, pp. 364–382, 2012.
- [22] T. Tarczewski, M. Skinski, L. M. Grzesiak, and M. Zieliński, "PMSM servo-drive fed by SiC MOSFETs based VSI," *Power Electron. Drives*, vol. 3, no. 1, pp. 35–45, 2018.
- [23] L. Paunonen and D. Phan, "Reduced order controller design for robust output regulation," *IEEE Trans. Autom. Control*, vol. 65, no. 6, pp. 2480–2493, Jun. 2020.
- [24] M. Goubey, A. Krejci, and J. Reitingner, "New virtual laboratories presenting advanced motion control concepts," *J. Phys.: Conf. Ser.*, vol. 659, 2015, Art. no. 012016.
- [25] T. N. Gücin, M. Biberoğlu, B. Fincan, and M. O. Gülbahçe, "Tuning cascade PI(D) controllers in PMDC motor drives: A performance comparison for different types of tuning methods," in *Proc. 9th Int. Conf. Elect. Electron. Eng.*, 2015, pp. 1061–1066.
- [26] C. Klarenbach, H. Schmirgel, and J. O. Krah, "Design of fast and robust current controllers for servo drives based on space vector modulation," in *Proc. PCIM Eur.*, vol. 17, pp. 182–188, May 2011.
- [27] V. Frago-Rubio, M. Velasco-Villa, M. A. Hernández-Pérez, B. del Muro-Cuellar, and J. Márquez-Rubio, "Prediction-observer scheme for linear systems with input-output time-delay," *Int. J. Control, Autom., Syst.*, vol. 17, no. 8, pp. 2012–2025, 2019.
- [28] S. Alcantara, C. Pedret, A. Ibeas, and R. Vilanova, "General smith predictors from an observer-controller perspective," in *Proc. IEEE Control Appl. Intell. Control*, 2009, pp. 1203–1208.



**Bartłomiej Ufnalski** (Senior Member, IEEE) received the M.Sc. and Ph.D. degrees in electrical engineering and the D.Sc. degree in automatic control and robotics from the Warsaw University of Technology, Warsaw, Poland, in 1999, 2005, and 2016, respectively.

Since 2017, he has been an Associate Professor with the Institute of Control and Industrial Electronics, Warsaw University of Technology. His research interests include automatic control in power electronics and drives, with emphasis on repetitive, nonlinear, and adaptive control algorithms for these systems.



**Lech Marian Grzesiak** (Senior Member, IEEE) received the M.Sc., Ph.D., and D.Sc. degrees in electrical engineering from the Warsaw University of Technology (WUT), Warsaw, Poland, in 1976, 1985, and 2002, respectively.

In 1977, he joined WUT, where he is currently a Full Professor and holds the position of Dean of the Faculty of Electrical Engineering. His research interests include applications of artificial intelligence in control systems, generally dedicated to adjustable-speed drives, servo drives, power electronic converters, and electrical energy generating systems.



**Marek Michalczuk** (Member, IEEE) received the M.Sc. and Ph.D. degrees in electrical engineering from the Warsaw University of Technology (WUT), Warsaw, Poland, in 2009 and 2017, respectively.

He is currently an Assistant Professor with the Institute of Control and Industrial Electronics, Faculty of Electrical Engineering, WUT. His research interests include automatic control in drives and power electronics.

Dr. Michalczuk was the winner of the 19th edition of the Fiat Chrysler Automobiles competition for the Best Doctoral Dissertation completed at the WUT.